Analysis of Asymmetrical Hot Strip Rolling by the Slab Method

Y.-M. Hwang and G.-Y. Tzou

Two analytical models based on the slab method are proposed to examine the behavior of sheet at the roll gap during the asymmetrical hot strip rolling process. In model I, the effect of shear stress in vertical plane at the roll gap is considered, whereas this effect is neglected in model II. Neutral points between rolls and strip, rolling pressure distributions along the contact art length of rolls, rolling forces, and rolling torques can be calculated easily by these proposed analytical models. The results including rolling pressure distributions, rolling forces, and rolling torques by both models are compared. The rolling pressure distribution predicted by model I shows that a "pressure well" develops in the cross shear region. On the other hand, no "pressure well" is predicted in model II. Furthermore, the rolling forces predicted by model I are always lower than those measured in the experiment, whereas those predicted by model II are always higher. However, the averages of the values predicted by model I and II are in fairly good agreement with the experimental data. Thus this analytical approach can offer useful knowledge in designing the pass schedules of the asymmetrical hot strip rolling processes.

Keywords

asymmetrical rolling, cross shear region, hot strip rolling, slab method

1. Introduction

MANY studies have been published (Ref 1-4) concerning symmetrical strip rolling, under which the peripheral velocity and radius of upper roll are equal to those of lower roll, respectively, since a uniform plastic deformation model of strip rolling was proposed by Orowan (Ref 5). Plastic deformation mechanism of the strip at the roll gap during symmetrical strip rolling has been made clear. Recently proposed is the asymmetrical strip rolling process, in which the rolling parameters, such as peripheral velocity, radius of upper roll, and so forth, may be different from those of the lower roll. This type of untraditional rolling process becomes more important because it has such advantages as less rolling pressure, less rolling force, less rolling torque, and better property of strip surface compared with symmetrical strip rolling. Most research related to the asymmetrical hot strip rolling are experimental investigations (Ref 6-10). A few works were carried out by a numerical method (Ref 11-13). Most of these studies, however, have not considered the effect of the shear stress at the roll gap or relied on the time-consuming numerical approach. Because the frictional coefficient between the rolls and sheet in cold strip rolling is relatively small compared to that in hot strip rolling, an analytical model using the slab method without considering the shear stress was presented by the present authors (Ref 14) to investigate the deformation mechanism of sheet at the roll gap during asymmetrical cold strip rolling. In this study, two analytical models are proposed. One considers the effect of shear stress in each slab element during asymmetrical hot strip rolling; the other does not. By this analytical approach, the rolling pressure distributions, rolling forces, and rolling torques can be obtained easily and quickly. The differences between the results obtained by these two models are compared. Effects of the various rolling parameters are systematically discussed; they are rolling speed ratio, thickness reduction, front and back tensions, and so forth., upon the rolling pressure distribution, rolling force, and rolling torque.

Y.-M. Hwang and **G.-Y. Tzou,** Department of Mechanical Engineering, National Sun Yat-Sen University, Kaohsiung, Taiwan 80424, Republic of China.

2. Mathematical Model

2.1 *Assumptions*

The formulation involved in developing the analytical models in asymmetrical hot strip rolling are simplified by employing the following assumptions:

- The rolls are rigid, and the strip being rolled is rigid, plastic material.
- The plastic deformation is plane strain.
- Stress are uniformly distributed within each slab element.
- Sticking friction occurs at the interface between the rolls and sheet; that is, the frictional shear stress, τ, is equal to the yield shear stress, k.
- The flow directions of strip at the entrance and exit of the roll gap are both horizontal.
- The total roll contact arc is small compared to the circumference of the roll.

These assumptions provide a physically realistic approximation for hot rolling processes of thin strip or sheet.

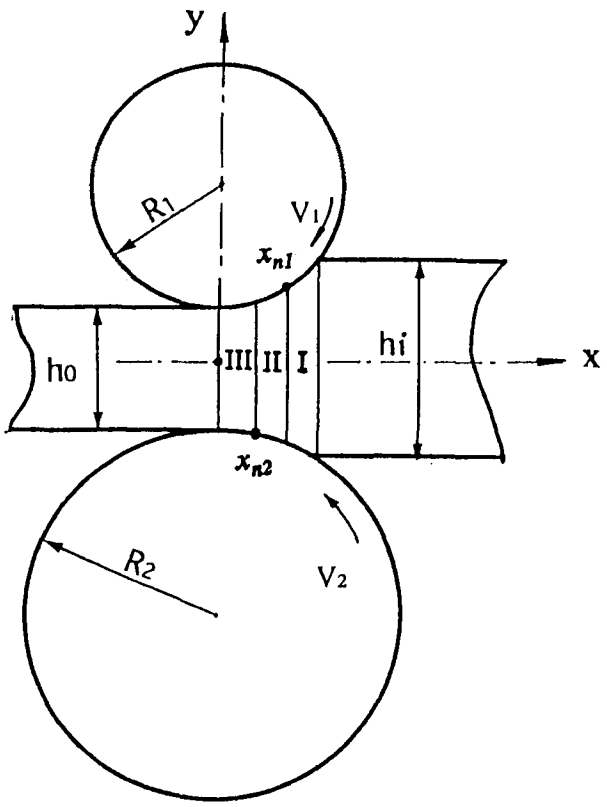

Fig. 1 Schematic illustration of the mathematical model

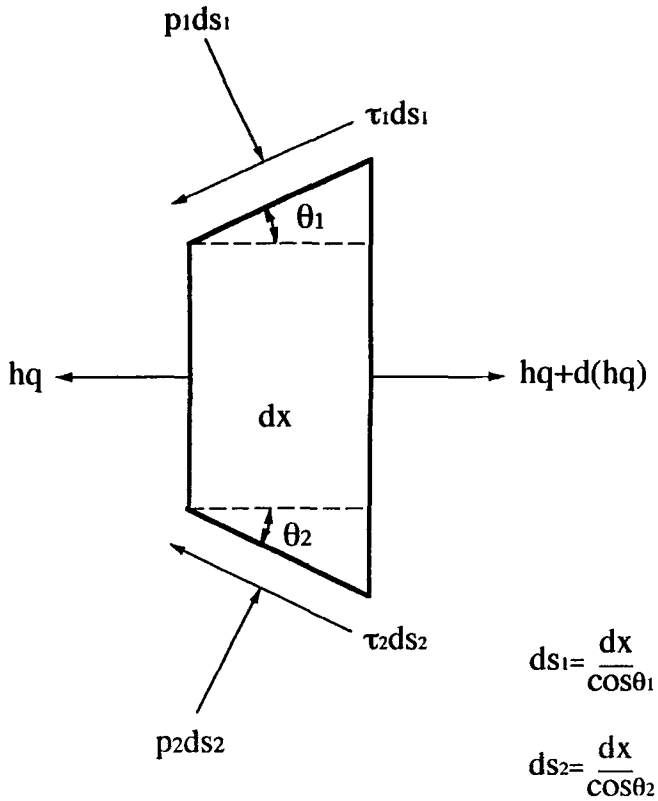

Fig. 2 Material element in zone I

2.2 *Formulation*

Figure 1 is the schematic illustration of asymmetric hot strip rolling. The radius and speed of the upper roll are different from those of the lower roll. The plastic deformation region at the roll gap is divided into three distinct regions according to the directions of frictional forces between the rolls and strip. These are denoted by zone I for the entry region, zone II for the cross shear region, and zone III for the exit region in Fig. 1. The subscripts 1 and 2 in all variables stand for the upper and lower rolls, respectively.

Figure 2 shows the stress state within a slab element in zone I, in which the directions of the upper and lower sticking frictional forces are both forward; that is, the velocities of both the upper and lower rolls are larger than that of the strip.

The mathematical expressions for the horizontal and vertical force equilibrium are summarized, respectively, as:

$$\frac{d(hq)}{dx} + p_1\tan\theta_1 + p_2\tan\theta_2 - (\tau_1 + \tau_2) = 0 \qquad \text{(Eq 1)}$$

and

$$P = p_1 + \tau_1\tan\theta_1 = p_2 + \tau_2\tan\theta_2 \qquad \text{(Eq 2)}$$

where q is the horizontal stress. h is the thickness at the roll gap; p_1 and p_2 are the specific rolling pressures of the upper and lower rolls, respectively; x is the horizontal distance from exit point of roll bite. $\theta_1(x)$ and $\theta_2(x)$ are contact angles of the upper and lower rolls at x cross section, respectively; τ_1 and τ_2 are sticking frictional stress along the upper and lower roll surfaces, respectively.

Combining Eq 1 and 2 gives:

$$h\frac{dq}{dx} + (p+q)\frac{dh}{dx} = \tau_1\frac{x^2}{R_1^2} + \tau_2\frac{x^2}{R_2^2} + \tau_e \qquad \text{(Eq 3)}$$

where

$$\frac{dh}{dx} = \frac{2x}{R_{eq}}$$

$$R_{eq} = \frac{2R_1R_2}{R_1 + R_2}$$

$$\tau_e = \tau_1 + \tau_2$$

τ_e is the effective sticking frictional stress, and R_{eq} is the effective radius.

The formulations derived above are specifically applied to both models as below.

2.2.1 Model I

According to the Prandtle compression theory of plate (Ref 15), the yield criterion of the sheet considering shear stress in zone I and III can be expressed as:

$$p + q = \frac{\pi k}{2} = Y \qquad \text{(Eq 4)}$$

where Y is the effective yield strength.

The yield shear stress, k, is expressed as:

$$k = \frac{\sigma_{yp}}{\sqrt{3}} \qquad \text{(Eq 5)}$$

where σ_{yp} is uniaxial yield strength.Refer to "Appendix A" for the detailed derivation.

The sticking frictional forces in zone II exerted by the upper and lower rolls are opposite in direction. The yield criterion in zone II based on the shearing compression slip line theory (Ref 16) is employed and expressed as:

$$p + q = k = Y \qquad \text{(Eq 6)}$$

Refer to "Appendix B" for the detailed derivation.

2.2.2 Model II

Traditionally, the shear stress in vertical plane is neglected; therefore, the von Mise's yield criterion in any zone can be expressed as $p + q = 2k$.

Because the procedures of derivation for both models are almost identical with each other, the derivation for only model I is described below.

Substituting Eq 4 or 6 into Eq 3 and rearranging it in dimensionless form, we obtain:

$$h\frac{dq}{dx} = \left(\frac{\tau_1}{R_1^2} + \frac{\tau_2}{R_2^2}\right)x^2 - Y\frac{2x}{R_{eq}} + \tau_e \qquad \text{(Eq 7)}$$

where

$$h = h_o + \frac{x^2}{R_{eq}}$$

h_o is the final strip thickness.

To solve Eq 7 by integration, we obtain:

$$q = Ax - \frac{B}{2}\ln(x^2 + D) - \frac{E}{\sqrt{D}}\tan^{-1}\frac{x}{\sqrt{D}} + c^* \qquad \text{(Eq 8)}$$

where

$$A = R_{eq}\left(\frac{\tau_1}{R_1^2} + \frac{\tau_2}{R_2^2}\right)$$

$$B = 2Y$$

$$C = R_{eq}\tau_e$$

$$D = R_{eq}h_o$$

$$E = DA - C$$

In zone I, where the directions of frictional force are all forward, that is., the strip velocity is smaller than that of upper and the lower rolls, the effective frictional stress, τ_e, is $2k$. Also, Eq 4 is valid ($Y = \pi k/2$). Likewise, in zone III, because the directions of sticking frictional force are all backward, that is., the strip velocity is larger than that of the upper and lower rolls, the form of the differential equation in zone III is the same as that in zone I. Only the effective sticking frictional stress, τ_e, is replaced by $\tau_e = -k - k = -2k$. In zone II, the sticking frictional forces are opposite in direction; accordingly, $\tau_e = -k + k = 0$. Also, Eq 6 is valid ($Y = k$).

2.3 *Boundary Conditions*

Because the horizontal position of the neutral point on the upper roll does not necessarily coincide with that on the lower roll, the direction of the sticking frictional force exerted by the upper roll on the strip is not necessarily the same as that by the lower roll. Assume that the velocity of the lower roll is larger than that of the upper roll, and the neutral points of the upper and lower rolls are denoted by x_{n1} and x_{n2}, respectively. The boundary conditions for the three distinct regions can be expressed as follows.

2.3.1 Zone III

$(0 \le x \le x_{n2})$, $\tau_e = -2k$; $p + q = \pi k/2$ at $x = 0$ (or $\omega = 0$),

$q = q_o$

$$q_o = -\frac{B_3}{2}\ln D + c_3^* \qquad \text{(Eq 9)}$$

where $B_3 = \pi k$ and q_o is the front tension exerted on the strip.

From the above boundary condition, the integral constant c_3^* can be obtained as:

$$c_3^* = q_o + \frac{B_3}{2}\ln D \qquad \text{(Eq 10)}$$

Hence, the horizontal stress (q_{III}) and the rolling pressure (p_{III}) in zone III can be expressed, respectively, as:

$$q_{III} = A_3 x - \frac{B_3}{2} \ln (x^2 + D) - \frac{E_3}{\sqrt{D}} \tan^{-1} \frac{x}{\sqrt{D}} + c_3^*$$

$$p_{III} = \frac{\pi k}{2} - q_{III} \qquad \text{(Eq 11)}$$

where

$$A_3 = -R_{eq} k \left(\frac{1}{R_1^2} + \frac{1}{R_2^2} \right)$$

$$C_3 = R_{eq} \tau_e$$

$$E_3 = DA_3 - C_3$$

2.3.2 Zone I

$(x_{n1} \le x \le L)$, $\tau_e = 2k$; $p + q = \pi k/2$ at $x = L$ (or $\omega = \omega_i = \tan^{-1} L/\sqrt{R_{eq} h_o}$), $q = q_i$

$$q_i = A_1 L - \frac{B_1}{2} \ln (L^2 + D) - \frac{E_1 \omega_i}{\sqrt{D}} + c_1^* \qquad \text{(Eq 12)}$$

where $B_1 = \pi k$, q_i is the back tension exerted on the strip, and L is the length of contact.

From this boundary condition, c_1^* can be expressed as:

$$c_1^* = q_i - A_1 L + \frac{B_1}{2} \ln (L^2 + D) + \frac{E_1}{\sqrt{D}} \omega_i \qquad \text{(Eq 13)}$$

where

$$A_1 = R_{eq} k \left(\frac{1}{R_1^2} + \frac{1}{R_2^2} \right)$$

$$C_1 = R_{eq} \tau_e$$

$$E_1 = DA_1 - C_1$$

Therefore, the horizontal stress (q_I) and the rolling pressure (p_I) in zone I are expressed as:

$$q_I = A_1 x - \frac{B_1}{2} \ln (x^2 + D) - \frac{E_1}{\sqrt{D}} \tan^{-1} \frac{x}{\sqrt{D}} + c_1^*$$

$$p_I = \frac{\pi k}{2} - q_i \qquad \text{(Eq 14)}$$

2.3.3 Zone II

$(x_{n2} \le x \le x_{n1})$, $\tau_{e=0}$, $p + q = k$ (in the case of $V_1 < V_2$). V_1 and V_2 are the rolling peripheral speeds of the upper and lower rolls.

Due to the continuity of boundary conditions at $x = x_{n2}$ (or $\omega = \omega_{n2}$) the horizontal stress (q_{III}) in zone III at $x = x_{n2}$ must be equal to that in zone II (q_{II}); that is, $q_{III} = q_{II}$. Accordingly, c_3^* and c_2^* have the relationship as follows:

$$A_3 x_{n2} - \frac{B_3}{2} \ln (x_{n2}^2 + D) - \frac{E_3}{\sqrt{D}} \tan^{-1} \frac{x_{n2}}{\sqrt{D}} + c_3^*$$
$$= A_2 x_{n2} - \frac{B_2}{2} \ln (x_{n2}^2 + D) - \frac{E_2}{\sqrt{D}} \tan^{-1} \frac{x_{n2}}{\sqrt{D}} + c_2^* \qquad \text{(Eq 15)}$$

where

$$A_2 = -R_{eq} k \left(\frac{1}{R_1^2} - \frac{1}{R_2^2} \right)$$

$$C_2 = 0$$

$$E_2 = DA_2 - C_2$$

Moreover, due to the continuity of boundary conditions at $x = x_{n1}$, that is., $q_I = q_{II}$, we obtain:

$$A_1 x_{n1} - \frac{B_1}{2} \ln (x_{n1}^2 + D) - \frac{E_1}{\sqrt{D}} \tan^{-1} \frac{x_{n1}}{\sqrt{D}} + c_1^* = A_2 x_{n1}$$

$$- \frac{B_2}{2} \ln (x_{n1}^2 + D) - \frac{E_2}{\sqrt{D}} \tan^{-1} \frac{x_{n1}}{\sqrt{D}} + c_2^* \qquad \text{(Eq 16)}$$

From Eq 15, c_2^* can be expressed as:

$$c_2^* = B^* x_{n2} + F^* \omega_{n2} + U^* \ln(x_{n2}^2 + D) + c_3^* \qquad \text{(Eq 17)}$$

where

$$B^* = A_3 - A_2$$

$$F^* = (E_2 - E_3)/\sqrt{D}$$

$$\omega_{n2} = \tan^{-1} \frac{x_{n2}}{\sqrt{R_{eq} h_o}}$$

$$U^* = \frac{1}{2} (B_2 - B_3)$$

$$B_2 = 2k$$

From Eq 16, c_2^* is also expressed as:

$$c_2^* = A^* x_{n1} + E^* \omega_{n1} + V^* \ln (x_{n1}^2 + D) + c_1^* \quad \text{(Eq 18)}$$

where

$$A^* = A_1 - A_2$$

$$E^* = (E_2 - E_1)/\sqrt{D}$$

$$V^* = \frac{1}{2}(B_2 - B_1)$$

V is the rolling peripheral speed. Substituting Eq 18 into Eq 17 then gives:

$$A^* x_{n1} + E^* \omega_{n1} + V^* \ln (x_{n1}^2 + D) + c_1^* - B^* x_{n2} - F^* \omega_{n2} - U^* \ln (x_{n2}^2 + D) - c_3^* = 0 \quad \text{(Eq19)}$$

where

$$\omega_{n1} = \tan^{-1} \frac{x_{n1}}{\sqrt{R_{eq} h_o}}$$

$$\omega_{n2} = \tan^{-1} \frac{x_{n2}}{\sqrt{R_{eq} h_o}}$$

To comply with the assumption of incompressibility, the positions of the upper and lower neutral points, x_{n1} and x_{n2}, have the following relationship.

$$x_{n1} = R_1 \sqrt{V_A \frac{x_{n2}^2}{R_1^2} + (V_A - 1)\frac{h_o}{R_A}} \quad \text{(Eq 20)}$$

where

$$V_A = \frac{V_2}{V_1}$$

$$R_A = \frac{R_1}{2}\left(1 + \frac{R_1}{R_2}\right)$$

Substituting Eq 20 into Eq 19, the solution of the neutral point, x_{n2}, can be determined easily using the bisection numerical method. Because x_{n2} is determined, x_{n1} and c_2^* can be obtained by Eq 20 and 17. Then, the horizontal stress and the rolling pressure, q_{II} and p_{II}, in zone II can be obtained as:

$$q_{II} = A_2 x - \frac{B_2}{2} \ln (x^2 + D) - \frac{E_2}{\sqrt{D}} \tan^{-1} \frac{x}{\sqrt{D}} + c_2^*$$

$$p_{II} = k - q_{II} \quad \text{(Eq 21)}$$

When c_1^*, c_2^*, and c_3^* are known from Eq 13, 17, and 10, respectively, the rolling pressures p_I, p_{II}, and p_{III} can be obtained by Eq 14, 21, and 11, respectively.

2.4 *Rolling Force*

The rolling force is determined by integrating the normal rolling pressure over the arc length of contact. Thus, the rolling force per unit width, P, is given by:

$$P = P_{III} + P_{II} + P_I \quad \text{(Eq 22)}$$

where

$$P_{III} = \int_0^{x_{n2}} p_{III} dx = III_1^* + III_2^* \quad \text{(Eq 23)}$$

$$III_1^* = -\frac{A_3}{2} x_{n2}^2 + \frac{B_3}{2} x_{n2} \ln (x_{n2}^2 + D) - \left(c_3^* + \frac{\pi k}{2}\right) x_{n2}$$

$$III_2^* = E_3 \left(\frac{\omega_{n2}^2}{2} + \frac{\omega_{n2}^4}{4}\right) + B_3 \sqrt{D}\, \omega_{n2}$$

$$P_{II} = \int_{x_{n2}}^{x_{n1}} p_{II} dx = II_1^* + II_2^* \quad \text{(Eq 24)}$$

$$II_1^* = -\frac{A_2}{2} x_{n1}^2 + \frac{B_2}{2} x_{n1} \ln (x_{n1}^2 + D) - (c_2^* - k) x_{n1} + B_2 \sqrt{D}\, \omega_{n1} + E_2 \left(\frac{\omega_{n1}^2}{2} + \frac{\omega_{n1}^4}{4}\right)$$

$$II_2^* = \frac{A_2}{2} x_{n2}^2 - \frac{B_2}{2} x_{n2} \ln (x_{n2}^2 + D) + (c_2^* - k) x_{n2} - B_2 \sqrt{D}\, \omega_{n2} - E_2 \left(\frac{\omega_{n2}^2}{2} + \frac{\omega_{n2}^4}{4}\right)$$

$$P_I = \int_{x_{n1}}^{L} p_I dx = I_1^* + I_2^* \quad \text{(Eq 25)}$$

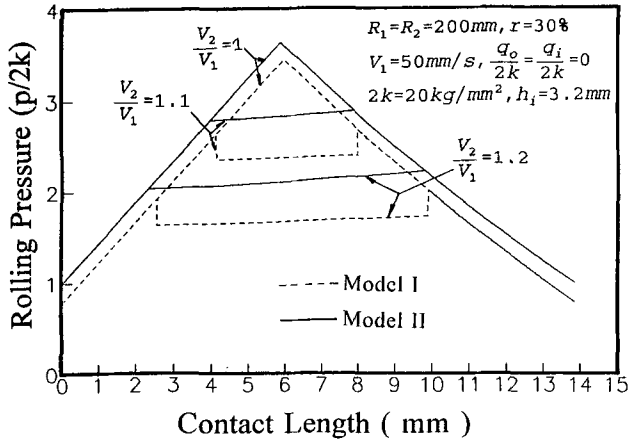

Fig. 3 Variation of the rolling pressures by models I and II with roll speed ratios

$$I_1^* = -\frac{A_1}{2}L^2 + \frac{B_1}{2}L\ln(L^2+D) - \left(c_1^* - \frac{\pi k}{2}\right)L + B_1\sqrt{D}\,\omega_i + E_1\left(\frac{\omega_i^2}{2} + \frac{\omega_i^4}{4}\right)$$

$$I_2^* = \frac{A_1}{2}x_{n1}^2 - \frac{B_1}{2}x_{n1}\ln(x_{n1}^2+D) - (c_1^* - \frac{\pi k}{2})x_{n1} - B_1\sqrt{D}\,\omega_{n1} - E_1\left(\frac{\omega_{n1}^2}{2} + \frac{\omega_{n1}^4}{4}\right)$$

2.5 *Rolling Torque*

The rolling torques, T_1 and T_2, exerted by the strip on the upper and lower rolls, respectively, can be calculated by integrating the moment of the sticking frictional force about the roll axis along the arc of contact. Therefore, the rolling torque of the upper roll is obtained as:

$$T_1 = R_1\left(-\int_0^{x_{n2}} k\,dx - \int_{x_{n2}}^{x_{n1}} k\,dx + \int_{x_{n1}}^{L} k\,dx\right) = R_1 k(L - 2x_{n1}) \quad \text{(Eq 26)}$$

The rolling torque of the lower roll is:

$$T_2 = R_2\left(-\int_0^{x_{n2}} k\,dx + \int_{x_{n2}}^{x_{n1}} k\,dx + \int_{x_{n1}}^{L} k\,dx\right) = R_2 k(L - 2x_{n2}) \quad \text{(Eq 27)}$$

The total rolling torque, T, needed is:

$$T = T_1 + T_2 \quad \text{(Eq 28)}$$

2.6 *Limiting Conditions for Successful Rolling*

Under the limiting conditions, both neutral points will be positioned inside the roll gap; accordingly, a successful rolling process can be implemented. For the purpose of finding the limiting conditions for roll speed ratio and reduction, let x_{n2} be 0 and $V_2 > V_1$. Then Eq 20 becomes:

$$x_{n1} = R_1\sqrt{(V_A - 1)\frac{h_o}{R_A}} \quad \text{(Eq 29)}$$

Substituting Eq 29 into Eq 19, the following relationship can be obtained:

$$A^*x_{n1} + E^*\omega_{n1} + V^*\ln(x_{n1}^2 + D) + c_1^* - U^*\ln D - c_3^* = 0 \quad \text{(Eq 30)}$$

In Eq 30, ω_{n1} is the function of x_{n1}, and x_{n1} is the function of V_A as shown in Eq 29. Thus, the limiting roll speed ratio, V_A, can be determined by the same procedures as those employed to determine the neutral point x_{n2} in Eq 19 and 20.

For the case with front tension, the front tension (q_o) is allowed only in a range such that x_{n1} is not out of the contact arc (i.e., $x_{n1} \le L$). The limiting value of q_o, for which x_{n1} reaches L, can be expressed as:

$$q_o = c_3^* - \frac{\pi k}{2}\ln D \quad \text{(Eq 31)}$$

where

$$c_3^* = A^*L + E^*\omega_i + V^*\ln(L^2+D) + c_1^* - B^*x_{n2} - F^*\omega_{n2}$$

$$x_{n2} = \frac{\sqrt{R_A L^2 - R_1^2(V_A - 1)h_o}}{R_A V_A} - U^*\ln(x_{n2}^2 + D)$$

The procedures for deriving neutral points, x_{n1} and x_{n2}, rolling pressure distributions, p, rolling force, P, and rolling torque, T, in model II are the same as those for model I. Only the effective yield strength is replaced by $Y = 2k$ in all zones.

3. Results and Discussion

Figure 3 shows the difference in rolling pressure between both models. The solid line indicates the results by model II in which the effect of shear stress is not considered at the roll gap, whereas the dashed line indicates the results by model I in which the effect of shear stress is considered. From the rolling pressure distribution predicted by model I, it is clear that: (a) a "pressure well" develops in the cross shear region (CSR), and (b) the CSR widens and the rolling pressure becomes less as the roll speed ratio, V_2/V_1, increases. Furthermore, (c) the rolling pressures predicted by model I are always lower than those by model II.

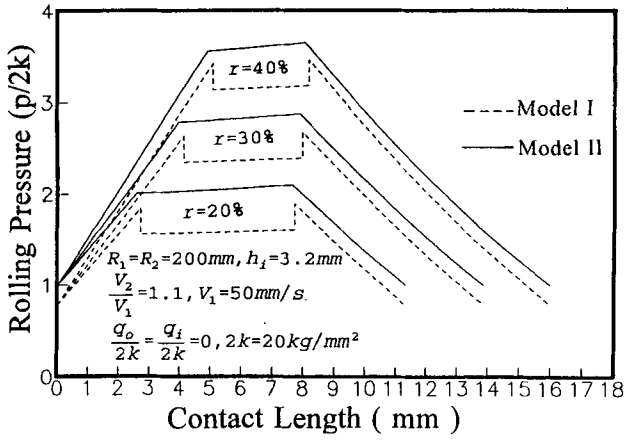

Fig. 4 Comparison of the rolling pressures by models I and II with various thickness reductions

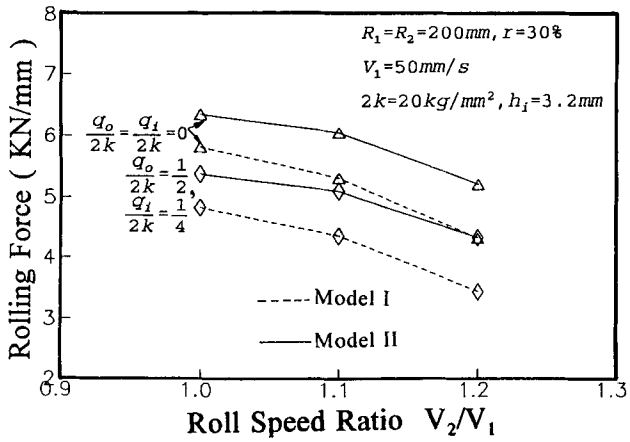

Fig. 5 Variation of rolling force with roll speed ratio for various front and back tensions

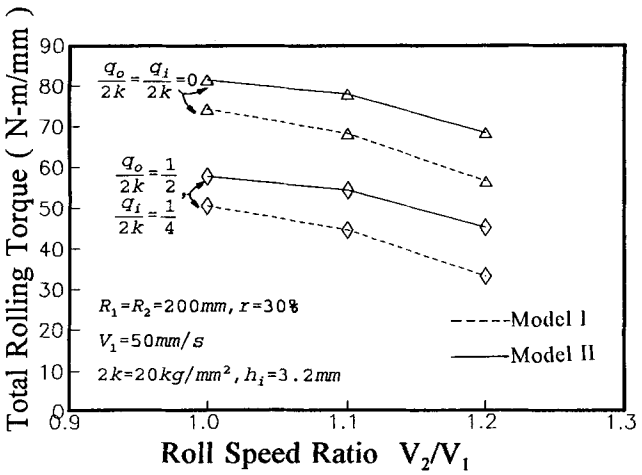

Fig. 6 Variation of total rolling torque with roll speed ratio for various front and back tensions

The variation of the distributions of the rolling pressure for different thickness reductions are demonstrated in Fig. 4. With increasing reduction, the rolling pressure increases, and the CSR becomes narrower. Moreover, the position of the CSR moves toward the entrance of the roll gap when reduction increases.

The effects of roll speed ratio, V_2/V_1, upon rolling force and rolling torque by both models are shown in Fig. 5 and 6, respectively. Rolling force and rolling torque are calculated by Eq 22 and 28, respectively. Evidently, both the rolling force and rolling torque decrease with increasing roll speed ratio. Rolling force also decreases with increasing front and back tensions. The rolling torque decreases with increasing difference between the front and back tensions when the former is larger than the latter. The rolling force and rolling torque by model I are lower than those by model II.

Figure 7 shows the effect of various R_{eq}/h_i ratios upon specific rolling pressures by both models. h_i is the initial strip thickness. The rolling pressure at the neutral point increases with larger ratios of R_{eq}/h_i. When $r = 30\%$, the limiting roll speed ratios, V_2/V_1, by model II are 1.375 and 1.355 for R_{eq}/h_i = 50 and 100, respectively. However, the corresponding roll speed ratios predicted by model I are 1.4 and 1.388, respectively. Note that the limiting roll speed ratios by model I are larger than those by model II. These analyses about limiting rolling conditions are necessary and important in asymmetrical hot strip rolling processes.

Figure 8 shows the effect of R_{eq}/h_i upon the limiting reduction, r, by both models. The limiting roll speed ratio V_2/V_1 increases with increasing R_{eq}/h_i. Although the contact length decreases with R_{eq}/h_i (R_{eq} is fixed), the rolling pressure distributions increase with increasing R_{eq}/h_i as shown in Fig. 7. Hence, the limiting roll speed ratio increases with increasing R_{eq}/h_i. Figures 7 and 8 show that as $r = 30\%$, the limiting roll speed ratios are V_2/V_1 = 1.355 and 1.375 for $R_{eq}/h_i = 50$ and 100, respectively, by model II. They are 1.388 and 1.4 by model I.

Figure 9 illustrates the effect of roll speed ratio, V_2/V_1, the reduction, r, upon limiting front tension, q_o. This illustration includes the cases of $x_{n2} = 0$ and $x_{n1} = L$. The case of $x_{n2} = 0$ means the neutral point, x_{n2}, reaches the exit of the roll gap before x_{n1} reaches the entrance of the roll gap, whereas the case of $x_{n1} = L$ means the neutral point, x_{n1}, reaches the entrance of the roll gap before x_{n2} reaches the exit. Under a fixed reduction and the condition of $x_{n2} = 0$, the limiting front tension, q_o, increases as the roll speed ratio, V_2/V_1, increases. As $x_{n2} = 0$ occurs, the limiting front tensions q_o are 0, 5 kg/mm^2, and 18.59 kg/mm^2, corresponding to V_2/V_1 = 1.2832, 1.3209, and 1.4278 for r = 30% by model II, respectively. As $x_{n1} = L$ occurs, the limiting front tension q_o increases under a fixed reduction with decreasing roll speed ratio. Note that the front tension cannot exceed $2k$, otherwise the fracture at the exit of the roll gap will occur. Consequently, only the limiting front tension under $2k$ is valid. By model I, with the conditions mentioned above, these limiting front tensions are 0, 5 kg/mm^2, 13.594 kg/mm^2, etc. The

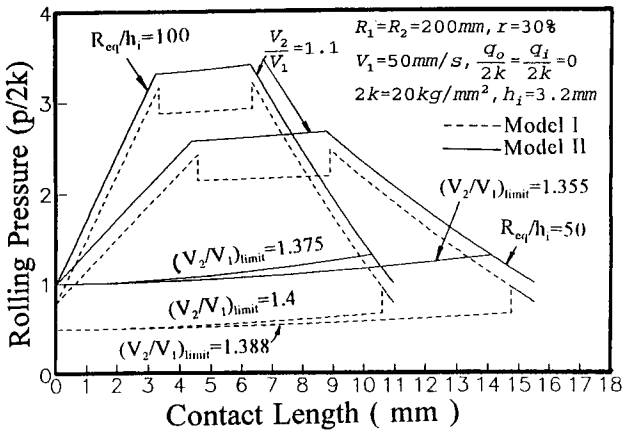

Fig. 7 Effect of various R_{eq}/h_i upon rolling pressure by model I and II.

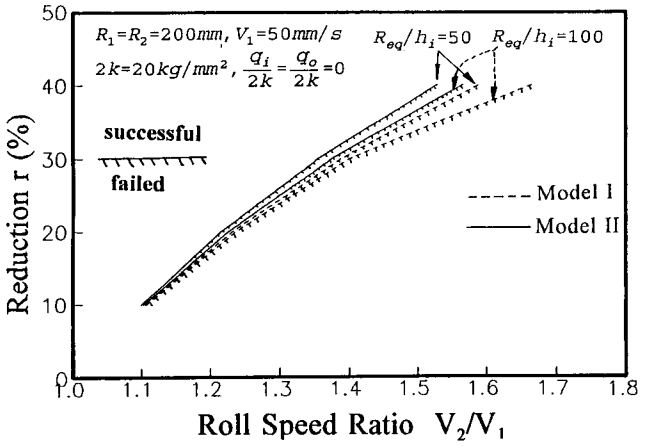

Fig. 8 Limiting reduction versus roll speed ratio for various R_{eq}/h_i (as $x_{n2} = 0$)

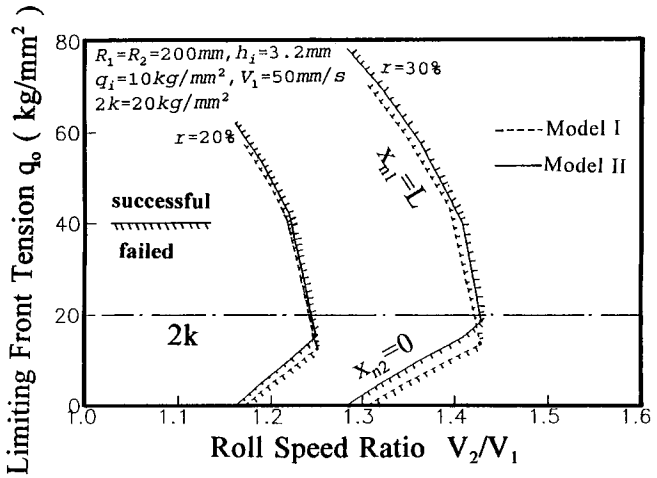

Fig. 9 Limiting front tension versus roll speed ratio for various reductions (as $x_{n1} = L$ or $x_{n2} = 0$).

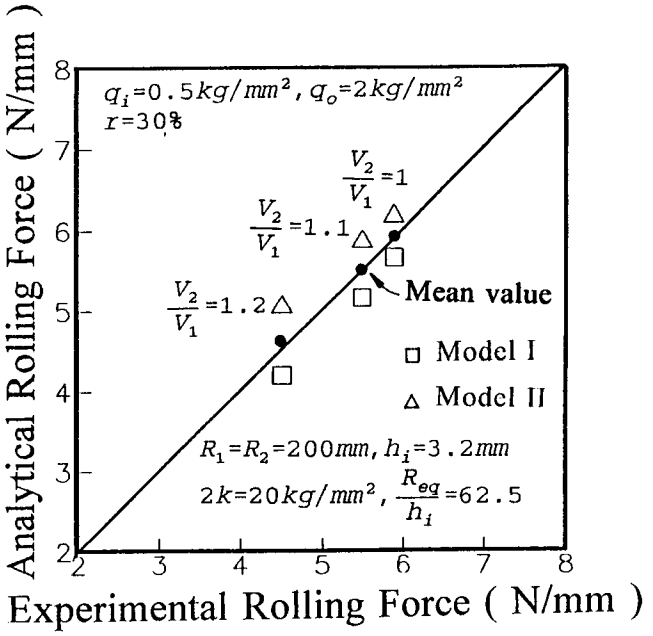

Fig. 10 Comparison of rolling forces between the theoretical predictions and experimental measurements

limiting front tensions by model I are smaller than those by model II under a fixed roll speed ratio as $x_{n2} = 0$ occurs, whereas the results are opposite to those as $x_{n1} = L$ occurs. Also, when the reduction, r, increases under a fixed front tension, the allowable roll speed ratio increases generally, because the rolling pressure distribution and the contact length become larger under a larger reduction.

The validity of this approach is verified by a comparison between the predicted rolling forces by both models and experimental measurements by Shiozaki (Ref 6), as shown in Fig. 10. The margin of error between the theoretical predictions and experimental measurements is approximately 15%. Note that the theoretical predictions by model I are always lower than experimental measurements, whereas those by model II are always higher than experimental measurements. In other words, if the effect of shear stress in each slab is taken into consideration, the predictions for rolling force are smaller than the experimental measurements. On the other hand, if the effect of shear stress is neglected, the predictions are larger than the experimental measurements. If we take the average value of the rolling forces calculated by models I and II, the predicted mean values are in good agreement with the experimental measurements as shown in Fig. 10.

4. Conclusion

This work provides an efficient analytical method to evaluate the rolling force and rolling torque based on two models. A few achievements obtained are summarized.

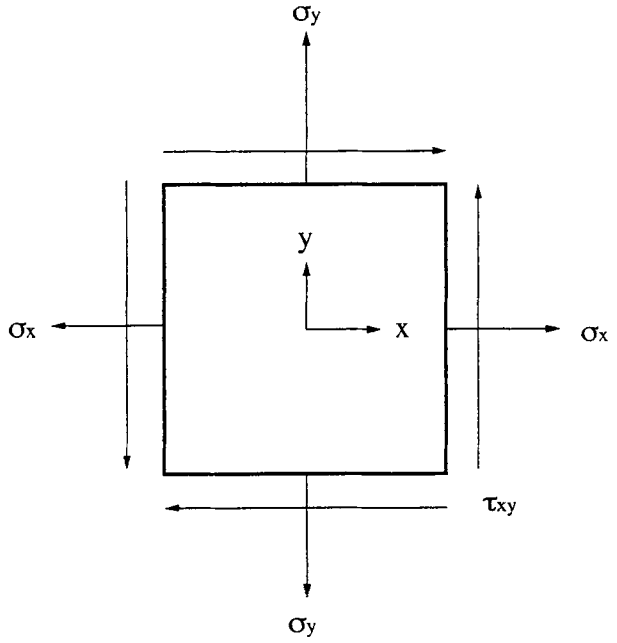

Fig. A1 Differential element for plane strain

- The rolling characteristics including rolling pressures, rolling forces, rolling torques, and limiting conditions obtained by using models I and II were compared.
- Both models illustrate that the rolling pressure and rolling force can be greatly reduced using asymmetrical rolling processes (i.e., $V_1 \neq V_2$).
- The limiting rolling conditions for the reduction, roll speed ratio, and front tension can be obtained readily. A successful asymmetrical rolling process can be ensured by controlling the rolling conditions under the limiting values.
- By this analytical approach, the rolling pressure distributions, rolling forces, rolling torques, and limiting rolling conditions can be obtained quickly in comparison with other numerical methods.
- Moreover, the rolling forces predicted by these models were compared with experimental results. If we take the average values of the rolling forces determined by models I and II, the predicted mean values are in good agreement with the experimental measurements.

5. Appendix A

Equation 4 is derived using zones I and III in model I.

The yield criterion considering the shear stress in a differential element (see Fig. A1) for plane strain can be expressed as:

$$\sigma_x - \sigma_y = 2k \sqrt{1 - \left(\frac{\tau_{xy}}{k}\right)^2} \qquad \text{(Eq A1)}$$

where σ_x is the horizontal normal stress, σ_y is the vertical normal stress, and τ_{xy} is the shear stress in the x-y plane.

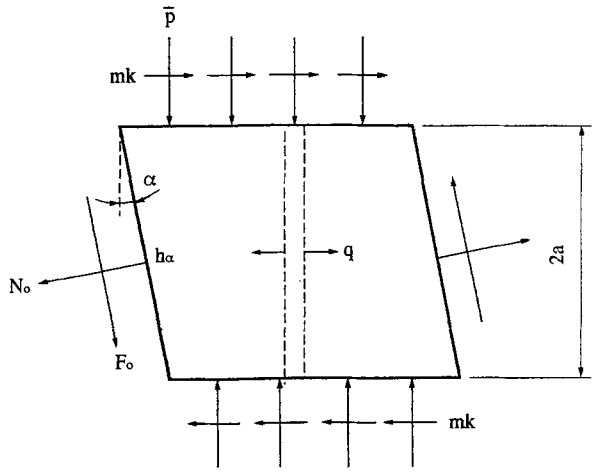

Fig. A2 Boundary conditions of plane strain shearing compression

Prandtle (Ref 15) assumes that the shear stress in vertical plane is linearly distributed. Thus, τ_{xy} can be expressed as:

$$\tau_{xy} = \frac{2k}{h} y \qquad \text{(Eq A2)}$$

Substituting Eq A2 into Eq A1 and integrating each term on both sides with respect to y gives:

$$\int_{-\frac{h}{2}}^{\frac{h}{2}} \sigma_x dy - \int_{-\frac{h}{2}}^{\frac{h}{2}} \sigma_y dy = \int_{-\frac{h}{2}}^{\frac{h}{2}} 2k \sqrt{1 - \left(\frac{2y}{h}\right)^2}\, dy \qquad \text{(Eq A3)}$$

Then, dividing each term by h, we obtain:

$$\frac{1}{h}\int_{-\frac{h}{2}}^{\frac{h}{2}} \sigma_x\, dy - \frac{1}{h}\int_{-\frac{h}{2}}^{\frac{h}{2}} \sigma_y\, dy = \frac{1}{h}\int_{-\frac{h}{2}}^{\frac{h}{2}} 2k \sqrt{1 - \left(\frac{2y}{h}\right)^2}\, dy \qquad \text{(Eq A4)}$$

The first term on the left side can be denoted by the uniform horizontal normal stress q. Also, the second term on the left side can be denoted by the uniform vertical normal stress p. Change the variable $2y/h$ in the term on the right side by sin θ. After the integration, we can finally obtain Eq 4 as follows.

$$p + q = \frac{\pi k}{2}$$

where

$$p = -\frac{1}{h}\int_{-\frac{h}{2}}^{\frac{h}{2}} \sigma_y\, dy$$

$$q = \frac{1}{h} \int_{-\frac{h}{2}}^{\frac{h}{2}} \sigma_x \, dy$$

6. Appendix B

Equation 6 is derived using zone II in model I.

Boundary condition of shearing compression for plane strain is shown in Fig. A2. Because the contact length in zone II (CSR) is much larger than thickness, generally slip line in zone II can be assumed as a straight line (refer to Ref 16). In Fig A2, N_0 and F_0 are the normal force and shear force applied to the edge plane of the strip, respectively. mk is the frictional shear stress applied to the upper plane of the strip, and p is the average normal stress applied to the lower plane. From the slip-line theorem (Ref 16), we get:

$$\frac{\bar{p}}{k} = 1 + \sqrt{1 - m^2} - N_{0,kh_\alpha} \qquad \text{(Eq A5)}$$

and

$$p = \bar{p} \qquad \text{(Eq A6)}$$

From the force equilibrium, we get:

$$q = \frac{N}{2a} = \frac{N_0 \cos\alpha - F_0 \sin\alpha}{h_\alpha \cos\alpha} \qquad \text{(Eq A7)}$$

where $2a$ is the thickness of the plate shown in Fig. A2.

Let $F_0 = 0$, then:

$$q = \frac{N_0}{h_\alpha} \qquad \text{(Eq A8)}$$

Substituting Eq A6 and A8 into Eq A5 then gives:

$$p + q = k(1 + \sqrt{1 - m^2}) \qquad \text{(Eq A9)}$$

In hot strip rolling, the surface frictional stress is assumed to be equal to the yield shear stress, k; i.e., $\tau_1 = \tau_2 = k$ and $m = 1$. Thus we obtain Eq 6:

$$p + q = k$$

Acknowledgment

This work was sponsored by the National Science Council of the Republic of China under grant No. NSC 81-0401-E-110-521. The advice and financial support of the National Science Council are gratefully acknowledged.

References

1. D. Rusia, Improvements to Alexander's Computer Model for Force and Torque Calculations in Strip Rolling Process, *J. Mater. Shaping Technol.*, Vol 8, 1990, p 167-177
2. D. Rusia, Review and Evaluation of Different Methods for Force and Torque Calculation in the Strip Rolling Process, *J. Mater. Shaping Technol.*, Vol 9, 1991, p 117-125
3. J.G. Lenard, Measurements of Friction in Cold Flat Rolling, *J. Mater. Shaping Technol.*, Vol 9, 1991, p 171-180
4. R.B. Sims, The Calculation of Roll Force and Torque in Hot Rolling Mills, *Proc. Inst. Mech. Eng.*, Vol 167, 1954, p 191
5. E. Orowan, The Calculation of Roll Pressure in Hot and Cold Flat Rolling, *Proc. Inst. Mech. Eng.*, Vol 150, 1943, p 140
6. H. Shiozaki et al., The Property of Asymmetrical Hot Strip Rolling, *Proc. of the 33rd Joint Conf. of JSTP*, Japan Society for Technol. of Plasticity, 1982, p 9 (in Japanese)
7. H. Yamamoto et al., Effects of Friction Coefficients on Asymmetrical Strip Rolling, *Proc. of the 34th Joint Conf. of JSTP*, Japan Society for Technol. of Plasticity, 1983, p 149 (in Japanese)
8. H. Shiozaki et al., Experimental Results of Asymmetrical Strip Rolling, *Proc. s-53 Sp. Conf. of JSTP*, Japan Society for Technol. of Plasticity, 1978, p 33 (in Japanese)
9. K. Nakajama et al., An Investigation of Rolling Property by Rolling Experiment in Asymmetrical Strip Rolling, *Proc. s-53 Sp. Conf. of JSTP*, Japan Society for Technol. of Plasticity, 1978, p 25 (in Japanese)
10. H. Shiozaki et al., Effect of Rolling Speed Ratio on the Rolling Force, Rolling Torque, Forward Slip in Cold Strip Rolling, *Proc. s-54 Sp. Conf. of JSTP*, Japan Society for Technol. of Plasticity, 1979, p 391 (in Japanese)
11. T. Kawanami et al., The Simplified Model of Asymmetrical Hot Strip Rolling, *Proc. s-57 Sp. Conf. of JSTP*, Japan Society for Technol. of Plasticity, 1982, p 61 (in Japanese)
12. H. Shiozaki and M. Mikami, Theory of the Different Work Roll Speed Rolling Based on the Slip Line Field Solution for the Shearing Compression of a Flat Plate, *J. JSTP*, Vol 24 (No. 264), 1983, p 37
13. H. Shiozaki et al., Study on the Rolling with Different Speed Ratio, *Proc. s-53 Sp. Conf. of JSTP*, Japan Society for Technol. of Plasticity, 1978, p 37 (in Japanese)
14. Y.M. Hwang and G.Y. Tzou, An Analytical Approach to Asymmetrical Cold Strip Rolling by the Slab Method, *J. Mater. Eng. Perform.*, Vol 2 (No. 4), 1993, p 597-606
15. L. Prandtle, *Z. Math. Mech.*, Vol 3, 1923, p 401
16. H. Shiozaki, Slip Line Field Solutions and Upper Bound Solutions for the Shearing Compression of a Flat Plate, *J. JSTP*, Vol 23 (No. 258), 1982, p 714